Resonance Control of a Weakly Resonating Supersonic Cavity Using Plasma Actuators

HONORS THESIS

In Partial Fulfillment of Honors Research Distinction for the Degree Bachelor of Science

at the Ohio State University

by

Dennis Omari

Undergraduate program in Aeronautical and Astronautical Engineering

The Ohio State University

2016

Undergraduate Examination Committee:

Dr. Mo Samimy, Advisor

Dr. James Gregory

Dennis Omari

2016

Abstract

Scramjets can provide efficient propulsion for aircraft flying at speeds greater than Mach 5. However, they are susceptible to engine unstart. Typically, thermal choking in the combustor is the cause of engine unstart. Unstart leads to loss of thrust and stalled engine operation. Isolators are generally employed to prevent unstart. The performance/stability of the scramjet engine operation could be increased by augmenting the isolator's unstart prevention capabilities. It is hypothesized that a resonating cavity imbedded in the isolator could supplement an isolator's capabilities by trapping the upstream travelling shock train to prevent unstart. The cavity geometry and Mach number determine the natural resonance state of the cavity. Since the Mach number will change in-flight, the cavity must be controlled to ensure it is resonating when needed. This study will assess the ability of plasma actuator to influence the resonance of a weakly resonating supersonic cavity. Investigation of various cavity geometries allowed for a cavity with a rounded trailing edge and a length to depth ratio of 4.4 to be selected for the desired weakly resonating case. Time resolved pressure data on the cavity floor, collected when actuation frequency was varied from below the 1^{st} Rossiter mode to above the 6^{th}, showed no resonance enhancement, so the frequency sweep was refined. Refined sweeps showed localized amplifications near the 4^{th} Rossiter frequency and its 1^{st} harmonic when excitation near the 4^{th} Rossiter frequency was introduced. This meant better shock trapping capabilities could be assessed at the 4^{th} Rossiter frequency and its 1^{st} harmonic. However, the effects of Electromagnetic Interference (EMI) must be reduced to improve the assessment. Therefore, further tests will be run to eliminate the effects of EMI. The shock trapping capabilities of the chosen cavity will be further assessed next using a shock generator.

Acknowledgements

For helping me throughout my studies at The Ohio State University, I would like to express my sincere appreciation to all my professors, co-researchers, friends, and family.

First and foremost, I would like to express my gratitude to my family for their immense support and guidance, without which this academic journey would not have been successful. I would like to thank my research advisor, Prof. Mo Samimy, for the opportunity to conduct research at the Gas Dynamics and Turbulence Laboratory (GDTL) at the Aerospace Research Center as well as all the assistance he provided throughout this project. I would also like to thank the Ohio Space Grant Consortium and the Undergraduate Research Program for providing funding that made this research possible.

Many thanks go to all of the students of the GDTL for their continued support and assistance in teaching me how to operate equipment at the research facility and improving my skills as a research scientist. I would like to give special thanks to Dr. Nathan Webb for all his assistance in conducting experiments, analyzing data, reviewing my literature and making sure I understand the procedures, concepts, and physics behind my results. I would like to commend Dr. Chris Clifford and Dr. Michael Crawley for their efforts in familiarizing me with different programming languages. Special thanks to Gregory Rhodes for his support and motivation throughout my journey.

Finally, I enjoyed working at the Aerospace Research Center in large part due to the faculty and students who also conduct different research in this facility. Thank you to everyone involved who made each day memorable.

Vita

2008 – 2012 ……..……. Diploma, Olentangy Orange High School

2014 ……..…. Undergraduate Researcher, Mississippi State University, Starkville, MS

2015…….. Undergraduate Researcher, The Ohio State University, Columbus, OH

2015 – 2016 ……..….. Research Fellow, The Ohio State University, Columbus, OH

Field of Study

Major Field: Aeronautical and Astronautical Engineering

Table of Contents

List of Tables

List of Figures

Nomenclature

PSD = Power Spectral Density

D = Cavity depth

h = Cavity ceiling displacement

L = Cavity Length

M = Freestream Mach number

n = mode number

P_a = Ambient Pressure

P_s = Static Pressure

SPL = Sound Pressure Level

St = Strouhal Number

U = Freestream Velocity

W = Cavity Width

β = Convective velocity of large-scale vortices, expressed as a fraction of the freestream velocity

ε = Phase lag between the intersection of a large scale structure in the shear layer with the cavity trailing edge and the formation of a corresponding upstream travelling disturbance

L/D = Length to Depth ratio

Chapter 1: Introduction

The importance of cavity flow control in the aerospace world has made it a constant topic of interest for the past 50 years. Its practical applications range from aircraft landing gear and weapons bays, to scramjet flame holders, and from the low subsonic to the supersonic flow regime. Large pressure fluctuations produced by cavity flow can lead to serious aerodynamic repercussions and mechanical failures (Webb and Samimy, 2015). For example, cavity flow can generate unwanted acoustic noise, in the landing gear of commercial aircraft. Therefore, controlling the pressure fluctuations within the cavity is desirable for improving aircraft performance.

When flow encounters a cavity, it separates from the leading edge of the cavity. The incoming boundary layer becomes the shear layer with upstream perturbations amplified generating acoustic tones at the trailing edge (Samimy et. all, 2007). The resonance caused by the pressure fluctuations can cause structural fatigue in the weapons bay of the aircraft. In addition to augmenting the acoustic field, it also modifies the flow field around the weapons bay, which can increase the drag of the cavity by 250% thereby affecting the performance and maneuverability of the aircraft (McGregor and White, 1970).

1.1: Scramjet Engine Unstart

Inlet unstart is a problem faced by scramjet designers. The heat released from combustion causes an increase in the back pressure, potentially leading to inlet unstart. Adding a cavity could increase the back pressure margin and therefore the stability and performance of the engine. The low pressure in the cavity, caused by entrainment, deflects the shear layer into the cavity,

accelerating the flow, and thereby trapping the shock. Figure 1 depicts a schematic of the scramjet engine with the inlet unstart occurring.

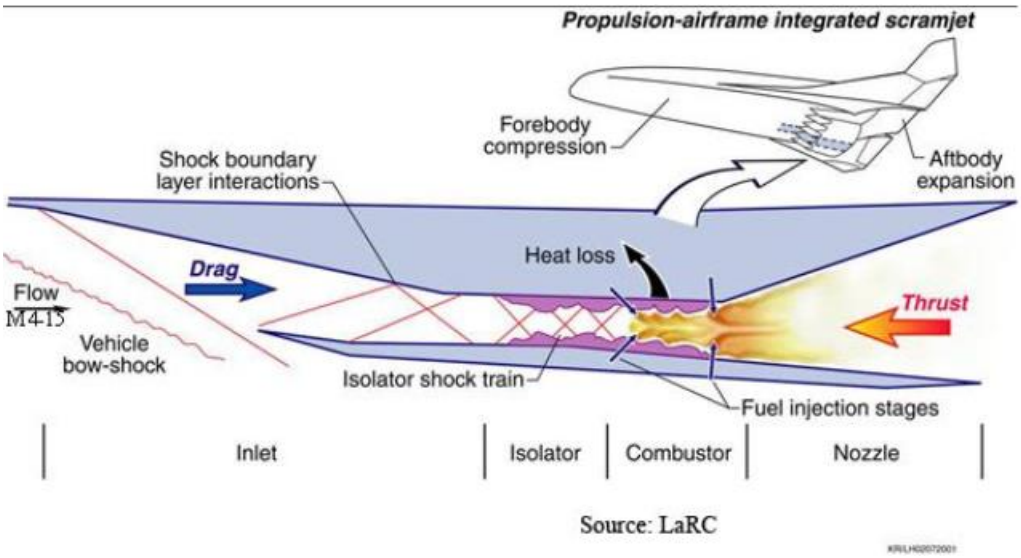

Figure 1: Schematic of Scramjet Engine (Ref. 15)

While a cavity may act as a shock trap, it also could impose a significant drag penalty. The drag penalty is caused by the shear-layer deflection associated with resonance. It is therefore desirable to suppress the cavity resonance during normal operation and then enhance resonance when necessary for shock trapping (Webb and Samimy, 2015).

Previously at the Aerospace Research Center, plasma actuators have been successfully used to control high subsonic flows for cavities with slanted aft wall (Yugulis et. al, 2013). Actuators introduce perturbations to the shear layer. These perturbations enhance the Kelvin-Helmholtz instability in the cavity flow, which can be tailored to enhance or suppress resonance. The plasma actuators consist of electrodes with a plasma arc forming when a high voltage is applied across them (Samimy et. al, 2007b). The plasma actuators will be used to enhance or suppress resonance in the supersonic cavity. During normal operation, the resonance will be suppressed; however, when imminent unstart is detected by a downstream sensor, the resonance will be

enhanced. This will provide a method of unstart prevention which gives significant back-pressure margin, while minimizing the drag penalty.

1.2: Cavity Flow Resonance

Cavity flow resonance occurs when cavities in the shear layer reattaches to the cavity aft wall instead of the cavity floor (Webb and Samimy, 2015). This leads to the cavity resonance forming a feedback loop. Incoming boundary layers possess some pressure fluctuations that perturb the origin of the shear layer that is most receptive to excitation (Webb and Samimy, 2015). These perturbations are amplified to large scale structures by the Kevin Helmholtz instability. Flo entrainment is caused by these structures, reducing the internal pressure, thereby deflecting the shear layer into the cavity. The interactions of the structures with the aft wall produce acoustic waves travelling to the shear layer, thereby completing the feedback loop ad establishing resonance.

Cavity flow can be characterized as an open, transitional, or closed cavity. Open cavities usually have a length to depth (L/D) ratio less than seven with boundary layer separation from the leading edge of the cavity. A shear layer is formed as a result of this separation and the resulting resonance generates strong tonal acoustic waves and broadband pressure fluctuations (Rossiter, 1996). Rossiter was the first to generalize a model for the cavity resonance, which is expressed in (Rossiter et. al, 1964) as:

$$St_n = \frac{f_n * L}{U} = \frac{n - \varepsilon}{M + 1/\beta}$$

Where n is the mode number, ε is an empirical constant associated with the phase delay in the acoustic generation process at the shear-layer cavity aft wall interaction region , β is an empirical constant with normalized convective velocity of large scale structures in the shear layer of the cavity, and M is the freestream Mach number.

The Rossiter model achieves good results in determining the Rossiter modes (resonant modes) from Mach number range of 0.4 to 1.4 but loses accuracy outside this range. Later, the equation was modified by Lawson and Barakos (2011), Heller et al. (1971) and Ahuja and Mendoza (1955) to account for the speed of sound inside the cavity being different from the freestream. This yielded:

$$St_n = \frac{f_n * L}{U} = \frac{n - \varepsilon}{M + \sqrt{\left\{\left(\frac{(\gamma - 1)}{2}\right) M^2\right\}} + 1/\beta}$$

Where γ is the specific heat ratio.

Figure 2 depicts the Power Spectral Density (PSD) of the pressure measurements for a baseline case. The dotted vertical black lines denote the expected Rossiter frequency mode, calculated using the Rossiter equation above. Typical Rossiter parameters used in literature are β=0.66 and ε=0.25 based on empirical data. Longitudinal modes of the cavity are related to the Rossiter modes. However, Debiasi and Samimy (2004) noticed an exception where the Rossiter modes aligned with the traverse modes.

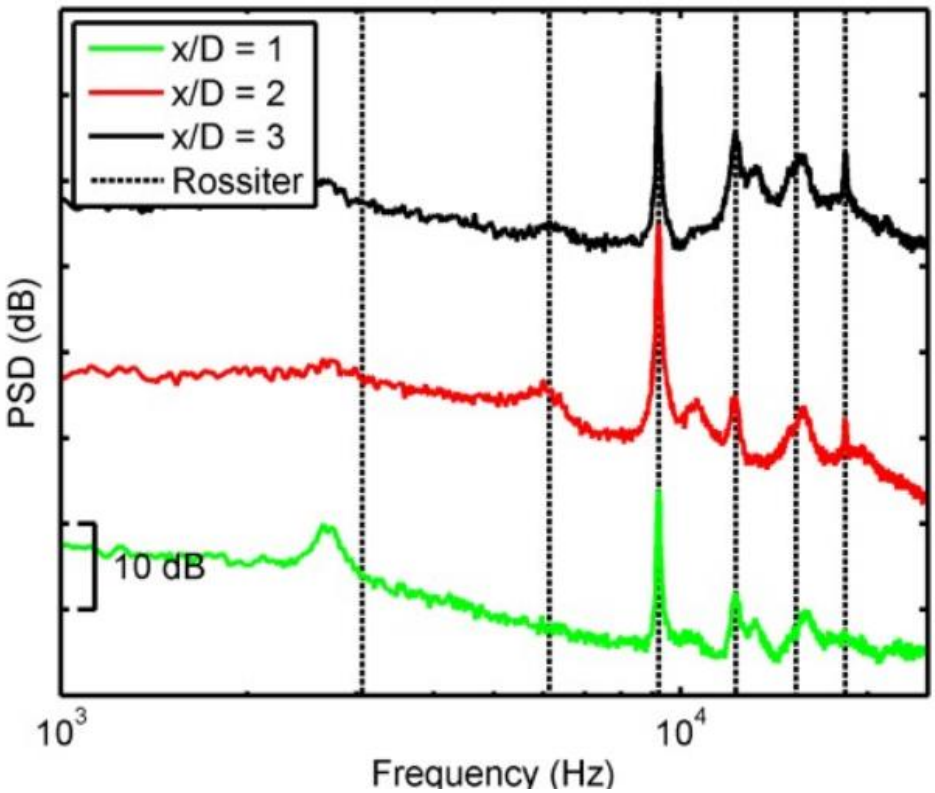

Figure 2: Mach 2.24 Cavity Flow Baseline PSD at Three Locations on the Cavity Floor (Webb and Samimy, 2015)

Mode switching is also present in open cavities. This occurs when the dominant resonance mode alternates between two or more Rossiter modes (Lawson and Barakos, 2011). When mode switching occurs, a time-accurate technique like wavelet analysis shows that two or more of the modes are strong but are only active for part of the time.

Closed cavities typically have L/D ratio greater than 10, with the shear layer reattaching to the cavity floor (Donbar et. al, 2010). The reattaching shear layer on the cavity wall leads to the high drag characteristics in cavities. Cavities with L/D between 7 and 10 are transitional and have interchangeable characteristics. Figure 3 depicts a schematic of an open cavity undergoing shear layer resonance.

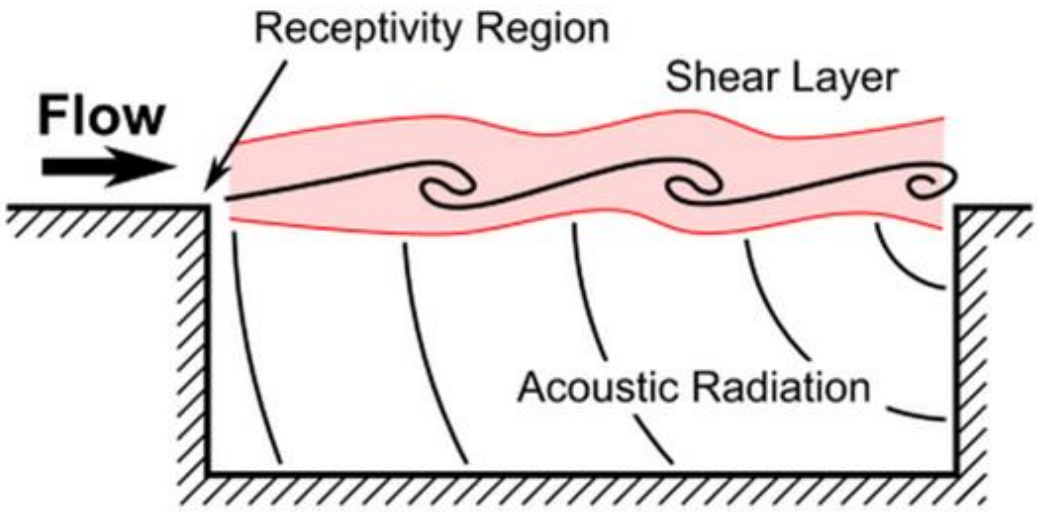

Figure 3: Open Cavity undergoing Rossiter Resonance (Webb and Samimy, 2015)

Cavity flow control has been a subject of interest due to its wide range of applications. There are two categories of flow control; namely passive control and active control. Passive control deals with geometric modifications that do not need external energy in the flow. Passive control is effective in reducing cavity tones, however, these modifications are usually permanent and as such, only effective at the design condition (Kegerise et. al, 2004). Passive control mechanisms are simple and inexpensive but usually generate high drag on the aircraft (Cattafesta et. al, 1997). Active flow control, on the other hand, adds energy to the flow, usually in the form of electrical, acoustic, or thermal energy. Active control is more complicated to implement but are often significantly more adaptable to changing conditions. The feedback control algorithms used in this project are useful to make active control devices more adaptable.

1.3: Plasma Actuators

Localized Arc Filament Plasma Actuators (LAFPAs) introduce perturbations that enhance natural instabilities, which generate structures. LAFPAs were developed to produce high frequency, strong amplitude perturbations to allow them to operate in subsonic, transonic and

supersonic flow. Previous studies have shown that LAFPAs are capable of enhancing resonance in a weakly resonating subsonic cavity (Webb and Samimy, 2015). Being able to control resonance will help minimize the drag penalty and optimize shock-trapping capabilities of the cavity in order to improve the engine performance. This control is implemented using the LAPFAs.

Due to the small power required to generate perturbations, the actuators use just tens of Watts each. Tungsten electrodes 1 mm in diameter are used and the electrodes in single actuators are separated by a center to center distance of 3.5 mm. Applying a sufficiently high voltage across the electrodes causes breakdown between the electrodes producing thermal and pressure perturbations (Samimy et. al, 2012). These are used to enhance natural instabilities in the flow. Figure 4 shows a physical configuration of two LAFPAs.

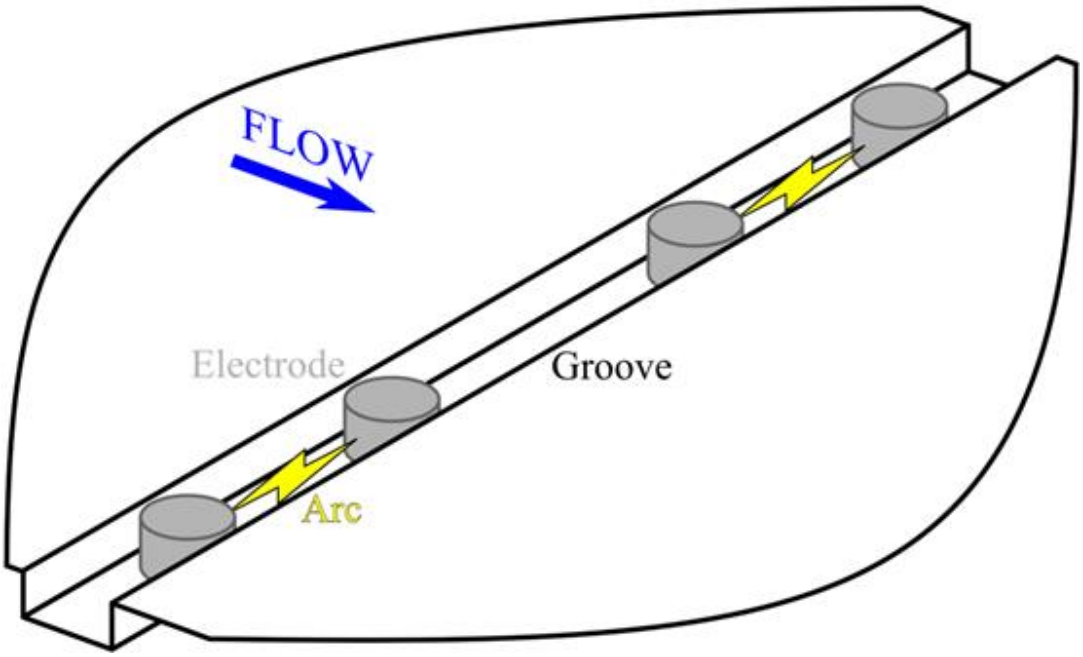

Figure 4: LAFPA Physical Configuration

As suggested in Webb and Samimy 2015, the correct location of the LAFPAs is vital to introducing perturbation that will enhance shear layer instabilities. This two dimensional instability that exists is most receptive to perturbations at the leading edge of the cavity (shear layer origin). Previous research work demonstrated perturbation control effectiveness when the actuators are placed at the leading edge of the cavity (Webb and Samimy, 2015). The LAFPAs exploit the flow configuration by exciting resonance in the cavity, and the actuators can't generate a resonance effect where no resonance exists. This is the reason why the project assesses the actuators' influence on the resonance of a weakly resonating supersonic cavity. Figure 5 shows the plasma actuator firing.

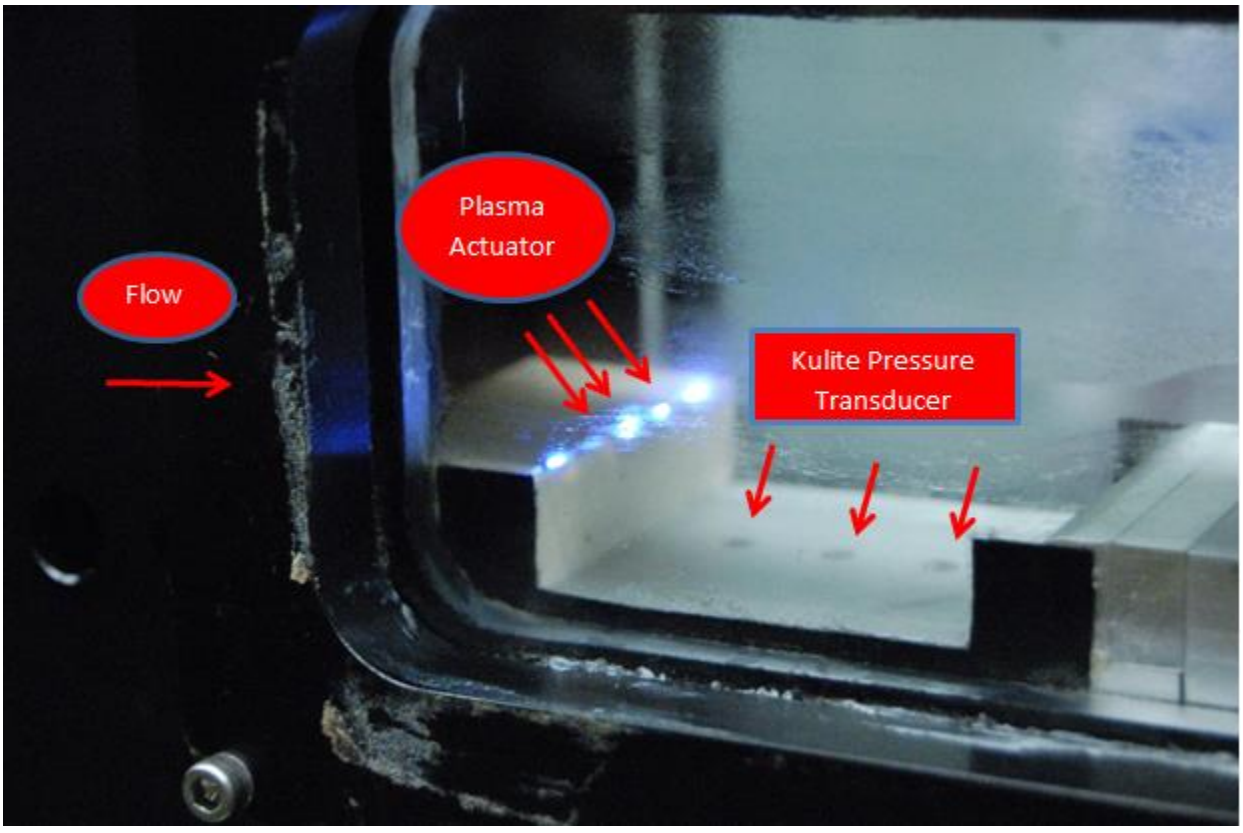

Figure 5: Plasma Actuator Firing to Control the Flow

Chapter 2: Experimental Arrangement

2.1: Facility

The supersonic wind tunnel used in this research was a blowdown facility at the Gas Dynamics and Turbulence Laboratory of the Aerospace Research Center at The Ohio State University. The supersonic wind tunnel was designed to allow many different cavity geometries to be tested. The facility is operated with air supplied from two high-pressure storage tanks with a total volume of approximately 36 m^3. The air is dried and filtered after compression. The air is directed through the stagnation chamber into two perforated plates and three turbulence-reducing screens before the converging section of the wind tunnel. A computer-controlled valve holds the pressure in the stagnation chamber constant while the facility is running. The stagnation pressure is constant to within 0.3% of the set pressure during a run. The stagnation temperature however, varies from 20^{o}C to -10^{o}C depending on the outdoor conditions, the tank pressure, and the run length. Figure 6 show an image of the supersonic wing tunnel used for the various experimental tests conducted.

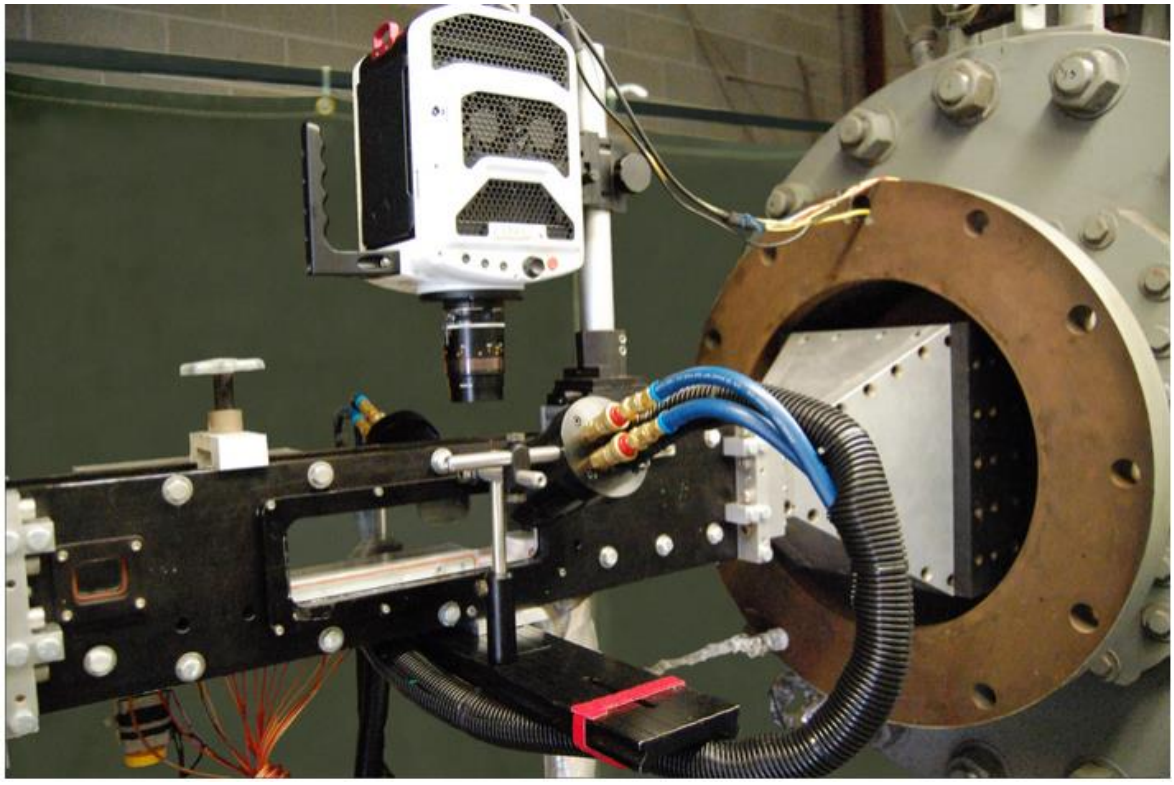

Figure 6: Supersonic Wind Tunnel at Aerospace Research Center

After exiting the stagnation chamber, the flow passes through a modular, contoured, converging/diverging nozzle, accelerating the flow to a freestream Mach number of about 2.24 in the test section. The test section measures 50.8 mm in height and 50.8 mm in width. As stated above the temperature varies through a run, however, the Reynolds number is approximately $Re_D \sim 6*10^5$. Optical access from both sides of the test section was provided by nominally 3 in. by 10 in. windows, and from top by a nominally 1 in. by 3.5 in. window. The windows are constructed from optical-grade fused silica to allow the transmission of high-intensity light if necessary during the course of the experiments.

The aft wall geometry was variable: vertical, rounded or slanted geometries could be installed. This research primarily uses rounded aft wall geometry because it produced fairly weaker resonance (as explained in Chapter 3). The cavity spanned the entire width of the test section.

The depth of the cavity was 12.7 mm; length was variable ranging from 48 mm to 64 mm, and thereby providing length to depth ratios from 3.78 to 5.04. Figure 7 shows a schematic of the side view of the cavity length on a rounded aft wall. The cavity length was varied in the test section using various rectangular shaped spacers of different lengths. Shorter cavity lengths meant more spacers stacked up together and longer lengths meant only one spacer was used.

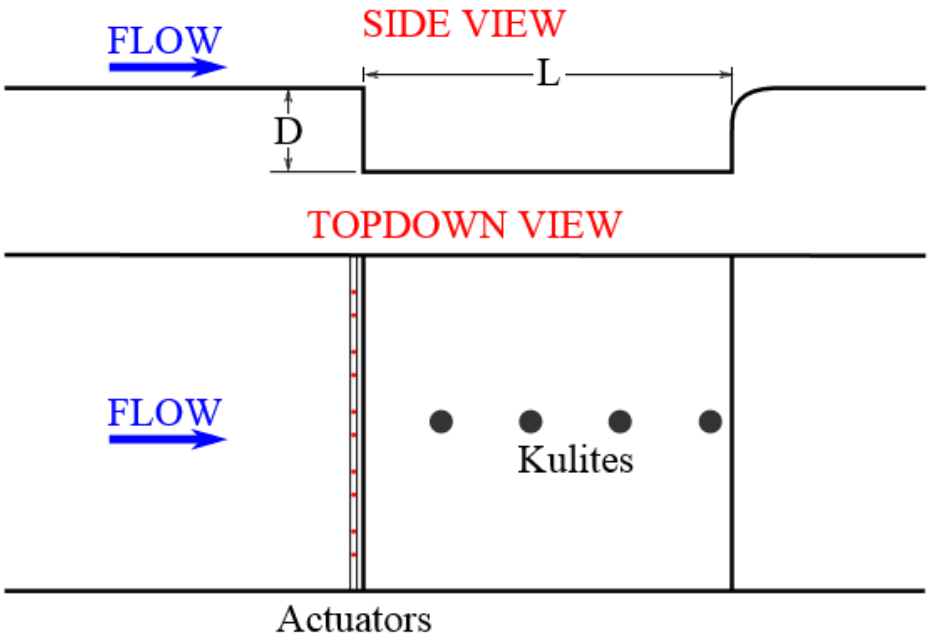

Figure 7: A Sample Cavity Layout

The plasma actuators (LAFPAs) are positioned as close to the leading edge of the cavity as possible (see Fig 5) to enable them to perturb the shear layer at its receptivity region (Little et. al, 2010). The actuators were arranged in a span-wise direction along the leading edge of the cavity. They were placed in a 1 mm wide by 0.5 mm deep groove. The trailing edge of the groove is 1 mm upstream the cavity edge. Five equally spaced actuators spanning the width of the wind tunnel were used throughout the research experiments. The LAFPAs are driven by computer-

controlled; transformer based high voltage power supplies. The power supply has the capability of driving the actuators at frequencies up to 20 KHz, providing a wide range of frequencies at which the flow can be enhanced. Each actuator can be individually controlled to allow various excitation modes both in phase and out-of-phase to be employed. The temperature perturbation by the plasma is one of the primary mechanism by which the LAFPAs introduce perturbations to the flow. Figure 5 shows plasma actuators being tested in the supersonic wind tunnel to assess its influence on the resonance of a weakly resonating cavity.

Time-resolved pressure measurements were the primary measurement techniques used in this research. Pressure transducers collected the Kulite data, which was then filtered at a frequency rate of 25 kHz, and was amplified using the plasma actuators. Kulite XTL-140-25A pressure transducers at the four centerline locations were used to collect static pressure (P_s) on the cavity floor. Figure 7 provides a visual depiction of the four Kulite pressure transducers. All data collected was sampled at a frequency of 75 KHz and low pass filtered at a frequency of 25 KHz to prevent aliasing. For collected case, 100 blocks of 4096 data points were collected and the power spectral density (PSD) was calculated and averaged over all blocks (Webb and Samimy, 2015). This provided frequency information about the cavity flow from 20 Hz to 25 kHz. The Mach number of the facility was confirmed to be 2.24. This was done by measuring stagnation pressure with a Pitot probe and the static with a pressure tap. Stagnation temperature was recorded using a thermocouple in the settling chamber. Schlieren images (from a standard Z-type apparatus) provided validation that the cavity flow was free of extraneous shocks.

Chapter 3: Cavity Geometry Search

3.1: Cavity Geometries

The described supersonic wind tunnel facility at the Gas Dynamics and Turbulence Laboratory of the Aerospace Research Center was used to search for optimal cavity geometry to assess the actuators' ability to enhance resonance in a weakly resonating cavity. A weakly resonating cavity was desired to determine if resonance could be enhanced by the plasma actuators. It was hypothesized that stronger resonance correspond to better shock trapping abilities of the cavity, thus resonance enhancement is an important part of this project. Data allowing the tonal peaks to be examined was used to select the optimal cavity geometry to demonstrate the resonance enhancement ability of the plasma actuators.

Time-resolved pressure acquisition as well as data acquisition programs were used throughout the experiments. Data acquisition programs are automated, which makes collecting data much easy and efficient. Different trailing edge cavity geometries were explored and once geometry was chosen, various cavity lengths were further explored to determine which would provide the best environment in which to assess the plasma actuators' abilities to enhance resonance in the chosen cavity. The trailing edge cavity geometries explored are listed in the table below:

Table 1: Trailing Edge Cavity Geometries

¼ round trailing edge cavity
½ round trailing edge cavity
45° slanted cavity
Straight/Rectangular cavity (90°)

The straight edge cavity (90° cavity) had been explored in a previous research and was demonstrated to produce a strong resonance in a weakly resonating cavity; hence the data collected for this cavity geometry was used for comparability and repeatability purposes. It was predicted a prior that the other three cavity geometries will produce weaker resonance because their ability to withstand back pressure weakened as the cavity geometry was modified from the straight/rectangular cavity. The cavity geometry search was the first phase of the research project because in order to prevent inlet unstart using a plasma controlled cavity, the LAFPAs ability to enhance resonance in the cavity needed to be explored, analyzed and optimized for better performance and efficiency. Figure 8 shows 3 pictures of different trailing edge cavity geometries explored.

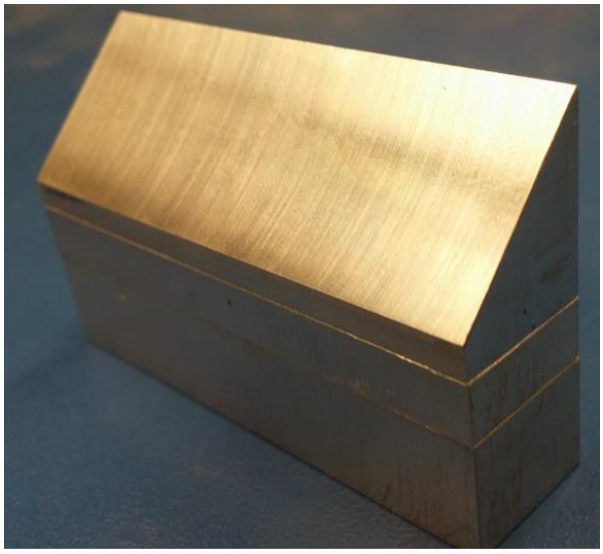

(a) 45° Angle

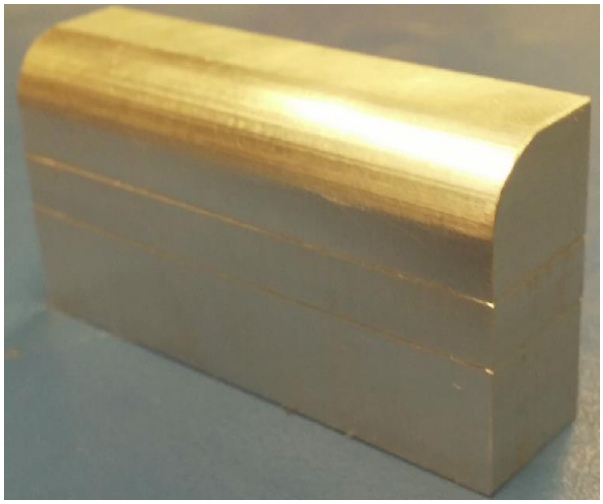

(b) ½ Rounded

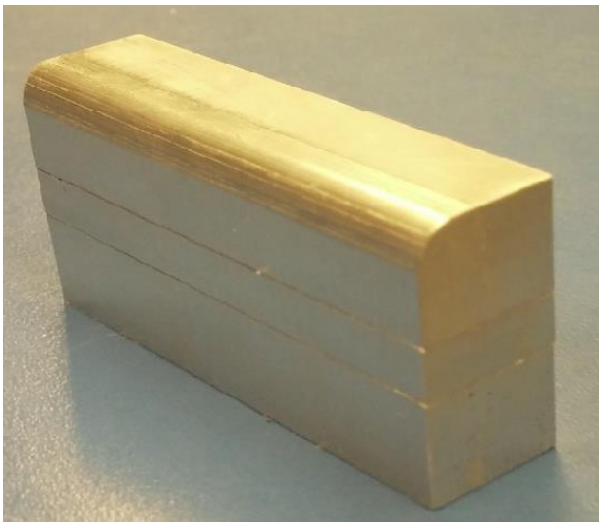

(c) ¼ Rounded

Figure 8: Photographs of Various Cavity Trailing Edge Geometries

3.2: Cavity Geometries Results

Kulite pressure transducers on the cavity floor were used to record cavity resonance and allow an appropriate, weakly resonating, geometry to be selected from all cavity geometries tested.

Experimental runs for each cavity geometry were conducted 3 to 4 times for repeatability. Figure 9 depicts the pressure spectral density plots for the three cavity geometries explored.

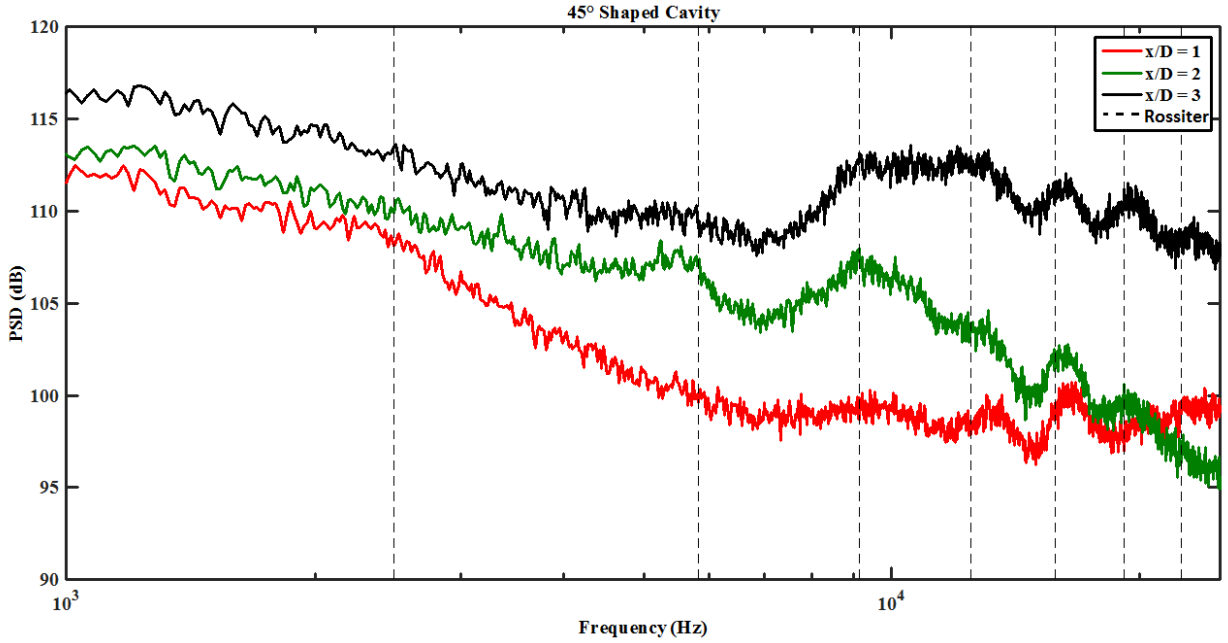

(a) 45° Trailing Edge

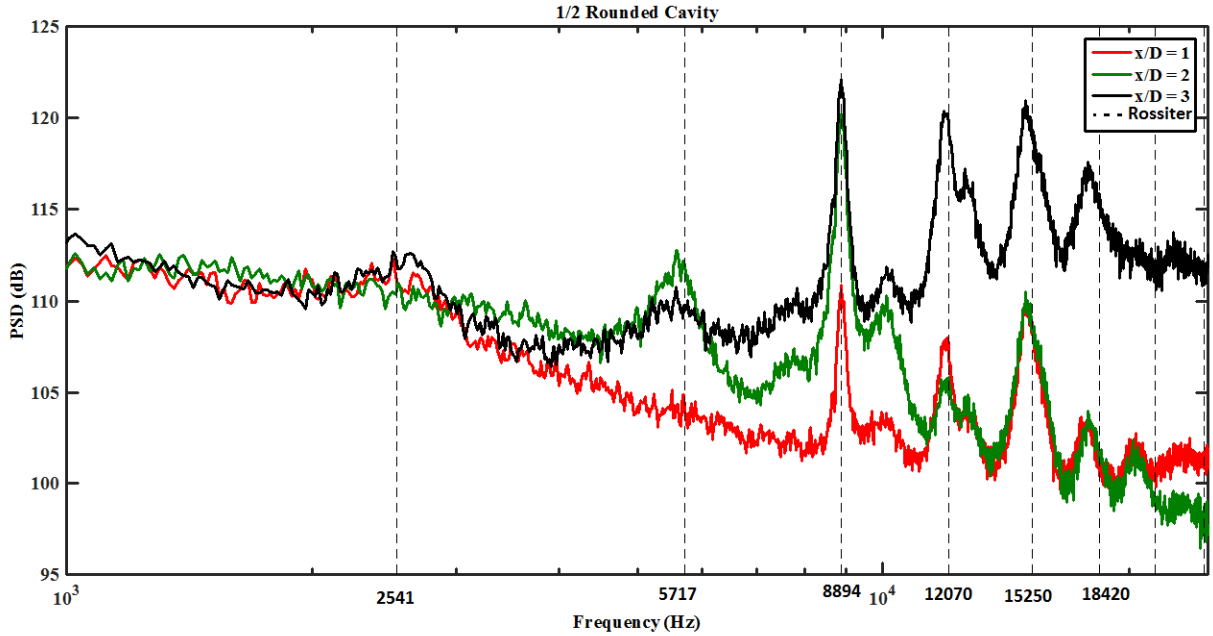

(b) ½ Rounded Trailing Edge

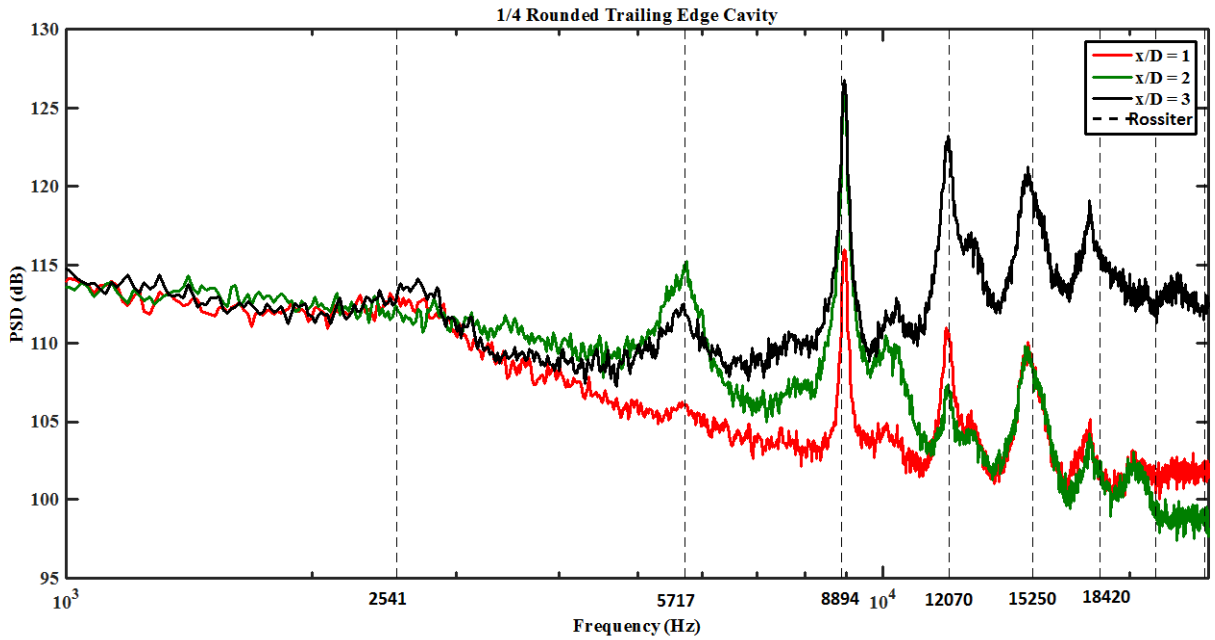

(c) ¼ Rounded Trailing Edge

Figure 9: PSD of Pressure Data for Baseline Cavity with L/D= 4

From the PSD plots, it can be observed that the 45° angled trailing edge cavity produced no resonance and the ¼ rounded trailing edge cavity resonated more strongly than the ½ rounded trailing edge cavity according to their tonal peaks. As demonstrated by the PSD plot above, the ¼ rounded trailing edge cavity and the ½ rounded trailing edge cavity resonated at the 3rd Rossiter mode. Table 2 below records the three different cavity geometries with their resonance peaks and frequencies.

Table 2: Resonance Peak

Cavity Geometry	Tonal Peak (dB)	Resonance Frequency (Hz)
¼ rounded trailing edge cavity	126.7	8936
½ rounded trailing edge cavity	122.5	8862
45° angled trailing edge cavity	_____	_____

From Table 2, the optimal cavity geometry that will allow for the assessment of the plasma actuators' influence of resonance on a weakly resonating supersonic cavity is the ½ rounded trailing edge. This is because it has the lowest resonance peak of the two cavities that resonated. Since previous research has shown that LAFPAs' can enhance resonance of a weakly resonating subsonic cavity, this research seeks to determine if the LAFPAs can have the same influence in the supersonic regime. A weakly resonating cavity was desired because the actuators cannot enhance resonance when there is no resonance or when there is a very strong resonance; therefore a balance of the two was desired. Hence a weakly resonating supersonic cavity was chosen for this research. This gave the plasma actuators some resonance to amplify but still allowed their abilities to enhance resonance to be clearly observed and documented. Once the ½ rounded cavity geometry was selected, the length of the cavity was adjusted to assess its influence on resonance. The cavity lengths explored ranged from 2.0 in to 2.5 in. Figure 10 shows an example of how the resonance strength was obtained for one cavity of one length. This figure shows the PSD for a cavity length of 2.3 in. As shown in the figure, the dominant Rossiter mode occurs at the 4^{th} Rossiter frequency. The relative amplitude of the 3^{rd} and 4^{th} Rossiter modes is close in magnitude and they both changed as length increased due to the overlap between the Rossiter equation and the longitudinal modes. Table 3 provides the full list of the cavity lengths normalized by cavity depth and corresponding resonance amplitudes as well as the dominant Rossiter mode in each case.

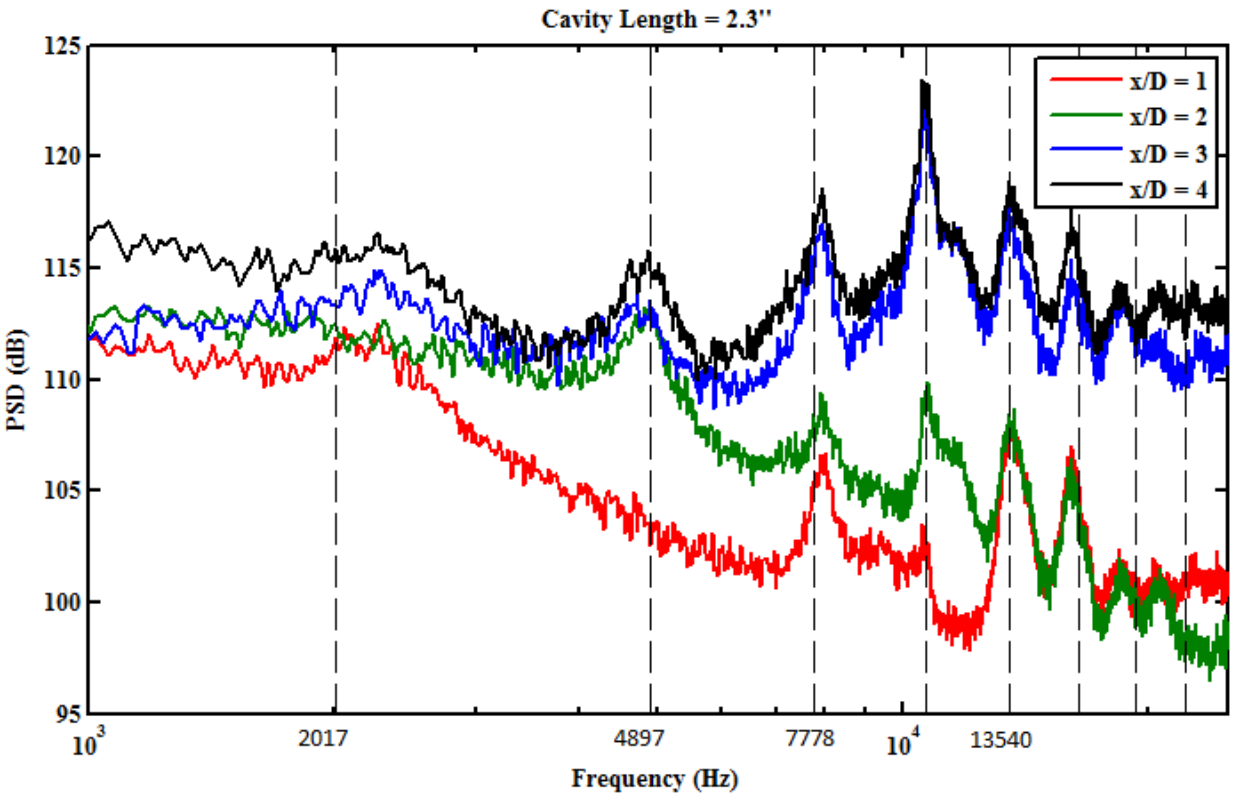

Figure 10: L=2.3 in

Table 3: Cavity Lengths, Resonance Amplitudes, and Associated Rossiter Modes

L/D	Tonal Peaks (dB)	Rossiter Mode
4.0	129.7	3rd
4.2	128.7	4th
4.4	126.3	4th
4.6	122.6	4th
4.8	120.4	4th
5.0	119.6	5th

The data shows that increasing the cavity length decreased the resonance strength, thereby decreasing the cavity's theoretical shock trapping ability. The Rossiter modes corresponding to

each peak frequency are tabulated to indicate where resonance is occurring and suggest potential operating frequencies at which the actuators may be able to enhance the existing resonance. It is interesting to point out that the Rossiter mode associated with the tonal peaks between the cavity lengths of 2.1 in to 2.4 in remained constant while that of 2.0 in and 2.5 in changed. As the length of the cavity increases, the overlap between the Rossiter modes and the longitudinal acoustic modes shifts the dominant Rossiter mode. As shown in Table 3, cavity lengths 2.1 in to 2.4 in showed no shift in the Rossiter modes because the change in acoustic mode frequency is not sufficient to jump to the 5th Rossiter mode, hence the resonance amplitudes remained at the 4^{th} Rossiter mode.

3.3: Optimization of Cavity Geometry

The results indicated that the resonance of the three different cavity geometries: ¼ rounded trailing edge, ½ rounded trailing edge, and 45° ramp trailing edge cavities matched the expected trends. The 45° angle trailing edge exhibited no sign of resonance. Since a weakly resonating supersonic cavity was desired, this geometry was not selected. The data showed the ¼ rounded trailing edge cavity resonated more strongly than the ½ rounded trailing edge cavity, hence, the ½ rounded trailing edge was the optimal geometry for this research project. The assessment of the resonance of ½ rounded trailing edge cavities of various lengths showed that increasing the cavity length decreased the resonance strength demonstrating that the plasma actuators could potentially have less cavity resonance enhancement with a decreased length. This is because decreasing the cavity length could lead to a much stronger resonance and increasing the cavity length tremendously will lead to a significantly weaker resonance that will not allow the actuators to have its intended effect. Due to these two extreme limits on the actuators, the

longest ½ rounded cavity length was not chosen because the plasma actuators needed some resonance to amplify, thus, an extremely weak resonance was not desirable. A longer cavity will produce a much weaker resonance which will make it difficult for the actuators to enhance resonance because there will be barely any resonance to enhance. Therefore, the ½ rounded trailing edge cavity with a length of 2.2'' (L/D = 4.4) was chosen as the optimal geometry to be used in the assessment of the plasma actuators' ability to enhance resonance.

Chapter 4: Actuated Measurements

4.1: Experimental Procedure

After verifying that a cavity with a rounded trailing edge (with a radius equal to half the cavity depth) and a length to depth ratio of 4.4 produced the desired weakly resonating condition, excitation from the LAFPAs was introduced. Actuated measurements were collected to assess the plasma actuators' ability to enhance resonance in a weakly resonating cavity. Assessing the plasma actuators' ability to successfully enhance resonance in the cavity is a step towards assessing the ability of the cavity to act as a shock trap. This is because it is essential that these actuators be able to enhance resonance when needed to trap unstart shocks.

35 baseline cases (actuators off) and 200 excited cases (actuators on) were collected during each experimental run. Before each run, the plasma actuators were tested briefly (via visual inspection) to verify they were functioning properly. The baseline cases were evenly interspersed with the excited cases to allow more accurate evaluation of any changes in the resonance and tonal peaks of the cavity. Data from the pressure transducers on the cavity floor was used to monitor the cavity resonance and to examine the effects of the LAFPAs on the cavity resonance.

4.2: Coarse Frequency Sweeps

The excitation frequency was varied from below the 1st Rossiter frequency to above the 6th Rossiter frequency, and time resolved pressure measurements on the cavity floor were collected to monitor the resonance of the weakly resonating supersonic cavity. Figure 11 shows the calculated Power Spectral Density (PSD) for the baseline and an enhanced case with frequency of 2 kHz respectively. As shown in this figure, the dominant resonance peak is the 4th Rossiter

mode with the tonal peaks after the 4th Rossiter mode having diminishing amplitudes. The PSD plot is shown for four channels collected at various streamwise locations normalized by the cavity depth. The high frequency hump from about 8 kHz to about 20 kHz has been a question of interest in the past but unfortunately nothing has been discovered about these humps. Previous research conducted by Webb et al. (Webb and Samimy, 2015) attempted to determine of the source of this hump, but no definitive cause was discovered.

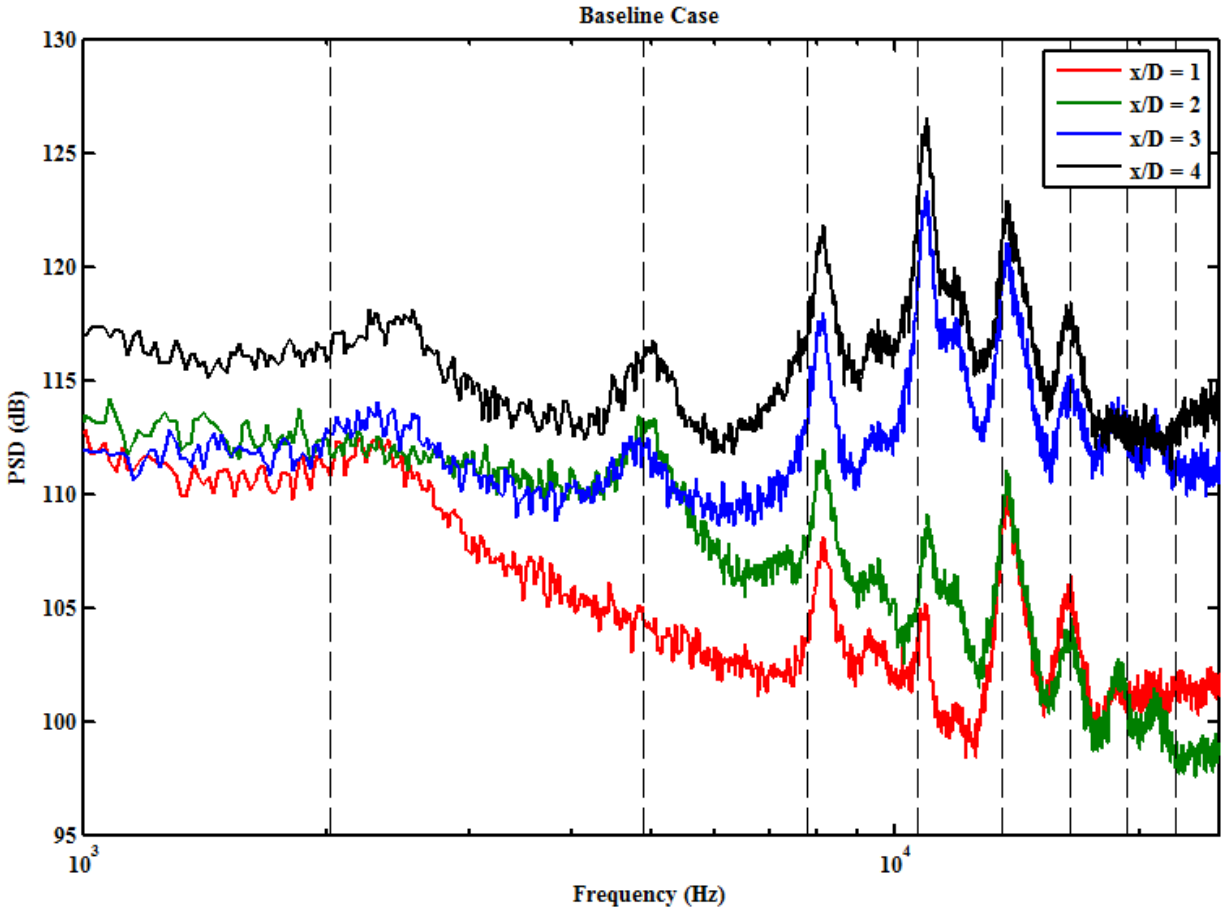

(a) Baseline Case

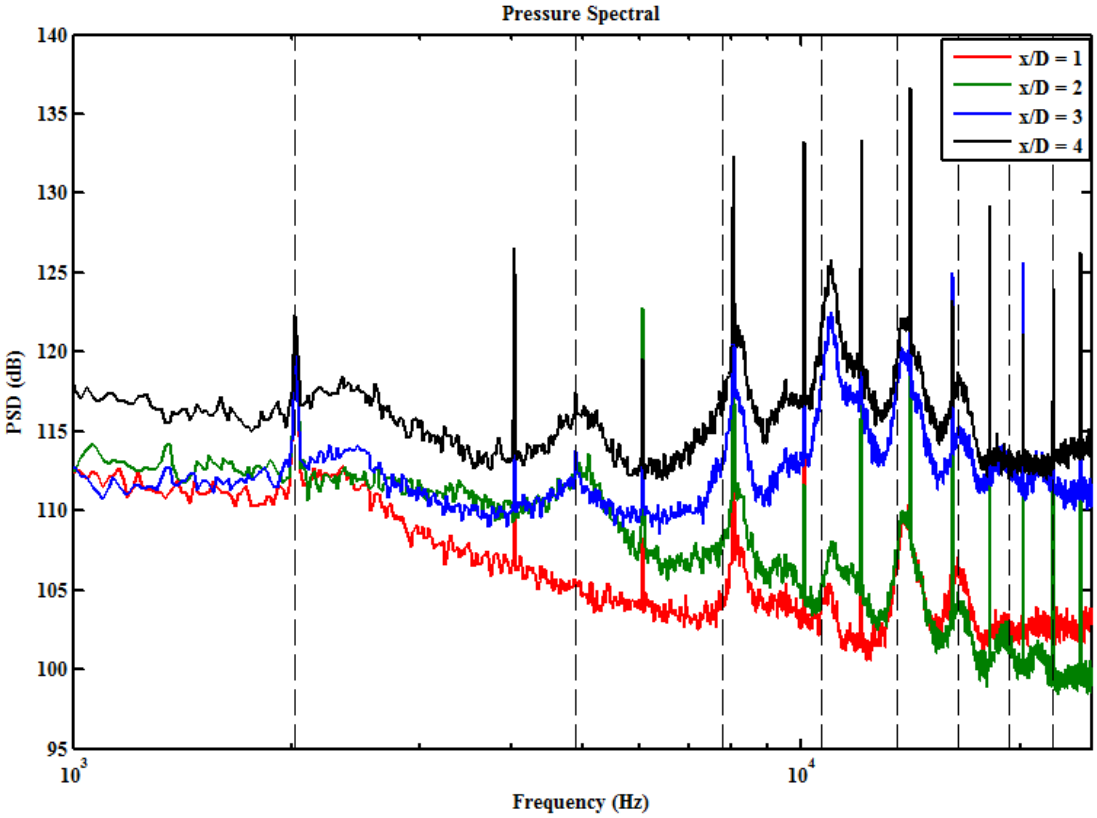

(b) Enhanced Case (f= 2 KHz)

Figure 11: Actuated Measurements for Baseline and Excited Case

The narrow spikes present in the PSD plot of the enhanced case are caused by Electromagnetic Interference (EMI) from the plasma actuators. This makes it difficult to analyze the cavity resonance since the EMI overlaps the resonance peak in some cases of interest. It is difficult to eliminate the EMI but measures were taken to control its effects by shielding the Kulite wires and the actuator power cables with aluminum foil. This reduced the EMI because the shield reduced the contamination of the signals and other devices by electrical noise. Since it could not be completely eliminated, this research acknowledges the presence of EMI and bears it in mind during the data analysis.

In order for the plasma actuators to enhance resonance in the cavity, there must be resonance present naturally. Data analysis showed that the frequency resolution of the initial (200 case) sweep was too coarse to observe any clear enhancement, making the assessment of the plasma actuators difficult, so the frequency sweep had to be refined. The original frequency sweeps were coarse too because the actuation frequency never matched the resonance frequency closely enough. Our working hypothesis suggests that the actuators will only enhance the resonance when the frequency matches closely with the natural resonance frequencies. Thus, a refined frequency sweep was necessary to more closely match the natural resonance frequencies. It is important to reiterate that the plasma actuators must reinforce the already present cavity resonance to enhance it in order to have its intended effect on the resonance. The refinement was confined to the area around a few selected frequencies at which weak resonance was naturally present. The plasma actuators cannot create resonance where there is none, hence, frequencies at which there is minimal natural resonance were not selected.

The frequencies of interest (around which the sweep was refined) were selected for the flow at a specific temperature. As the experiments progressed, the wind tunnel cooled due to the flow expanding from the tanks and accelerating through the test facility causing the flow temperature to decrease. To account for this variation, a temperature profile for the run was pre-determined and the frequencies adjusted accordingly. The predicted Rossiter Strouhal number remains constant with respect to temperature but predicts that the frequency will change with respect to temperature. From the equation for Strouhal number,$St = \frac{f*L}{U_\infty}$ since the Strouhal number and cavity length are constant, the frequency over the free stream velocity; $\frac{f}{U_\infty}$ will also be constant

with respect to the initial temperature. The constant relationship allows the refined frequency f_2 to be expressed below as:

$$\frac{f_1}{U_1} = \frac{f_2}{U_2} => \ f_2 = \frac{U_2}{U_1} * f_1 \qquad (1)$$

The ratio of the freestream velocities serves as a conversion factor to correct for the refined frequency. With the relationship between freestream velocity and Mach number below, it can be demonstrated that the freestream velocity is proportional to the square root of the stagnation temperature.

$$U_\infty = \sqrt{\gamma * R * T_{01} * (1 + \frac{\gamma - 1}{2} * {M_\infty}^2)} \qquad (2)$$

Where γ= ratio of specific heats, R= Universal gas constant and M_∞= Mach number. Expressing the freestream velocities as a function of temperature multiplied by a constant; C yields;

$$\frac{U_2}{U_1} = \frac{C * \sqrt{T_{02}}}{C * \sqrt{T_{01}}} = \frac{\sqrt{T_{02}}}{\sqrt{T_{01}}} \qquad (3)$$

Therefore replacing the ratio of freestream velocities in the equation for the refined frequency search yields;

$$f_2 = \sqrt{\frac{T_{02}}{T_{01}}} * f_1 \qquad (4)$$

The only parameter left to be determined is T_{02}.

Each experiment took approximately two hours to complete. The variation in temperature was recorded during the coarse sweeps and this variation was used to predict the temperature profile

for the refined runs. The frequencies of interest specified for the refined sweep are listed in Table 4.

Table 4: Refined Frequencies

Rossiter Mode	Frequency (Hz)
1	2430
2	5160
3	8339
4	11272
5	14212
6	16847

4.3: Frequencies of Interest

This refined frequency sweep tested 200 frequencies evenly spaced in log space overlaid by regions of interest of ± 500 Hz centered around the frequencies of interest with 50 cases (evenly spaced in log space). Two hour long experimental runs were conducted for the refined frequency sweeps with 50 baseline cases interspersed with 288 enhanced cases. Honing in on specific frequencies made it possible to assess the resonance changes in the cavity when the actuator frequency matched (more precisely) the naturally present frequency. Figure 12 shows the baseline cases and excitation at the 1^{st} – 6^{th} Rossiter frequency. The result of introducing excitation at these Rossiter frequencies demonstrate which specific Rossiter mode(s) the actuators were able to enhance. EMI makes it is very difficult to determine what portion of the

peak at the excitation frequency is EMI and what the actual flow response is. In Figure 12b, EMI overlaps the 1st Rossiter mode.

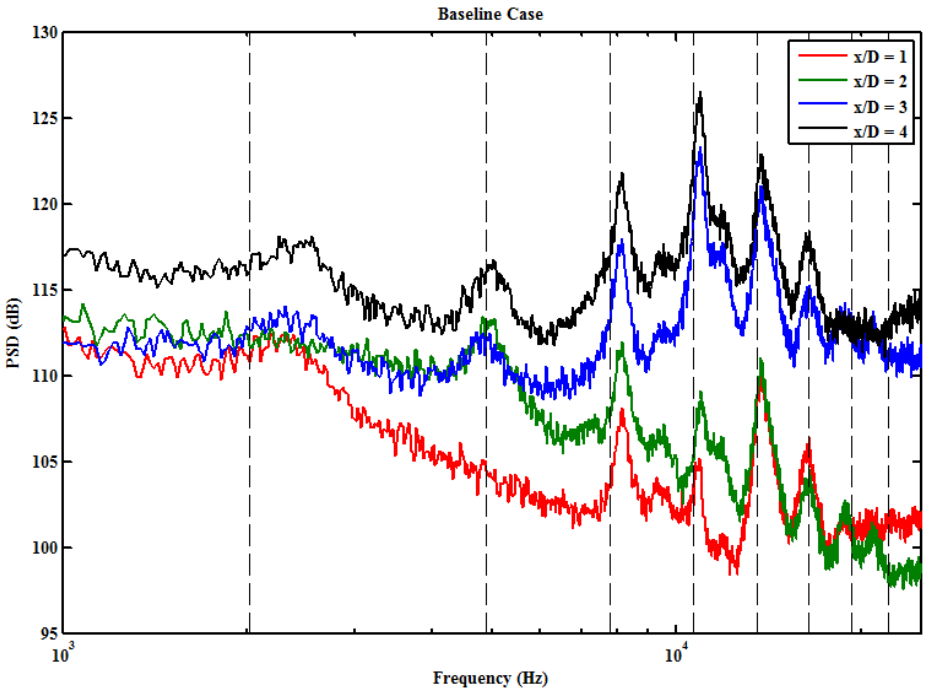

(a) Baseline Case

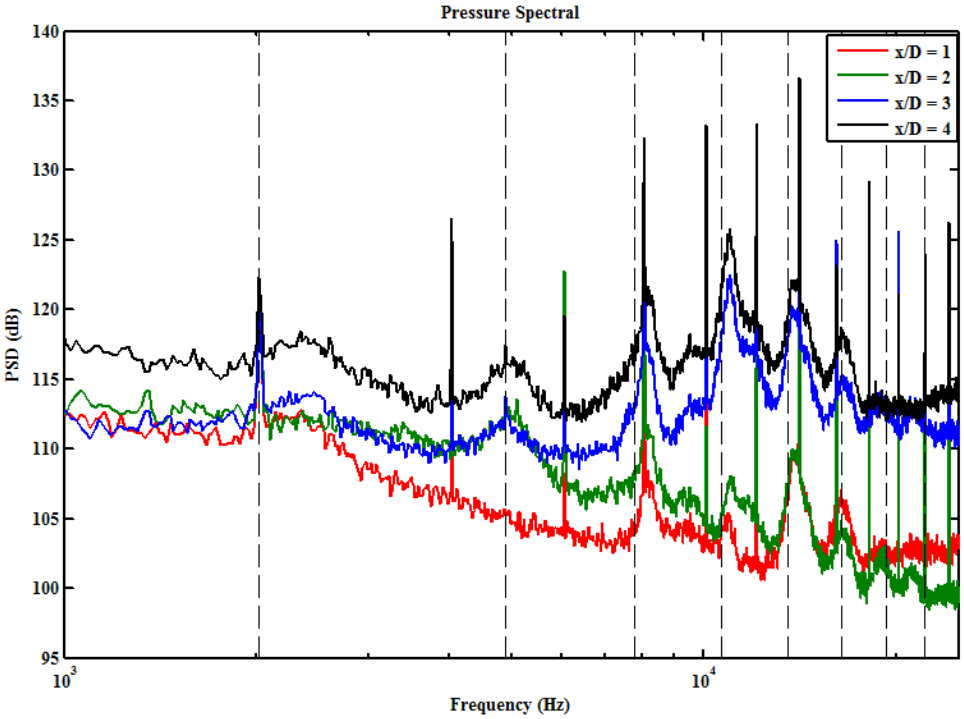

(b) 1st Rossiter Frequency Excitation

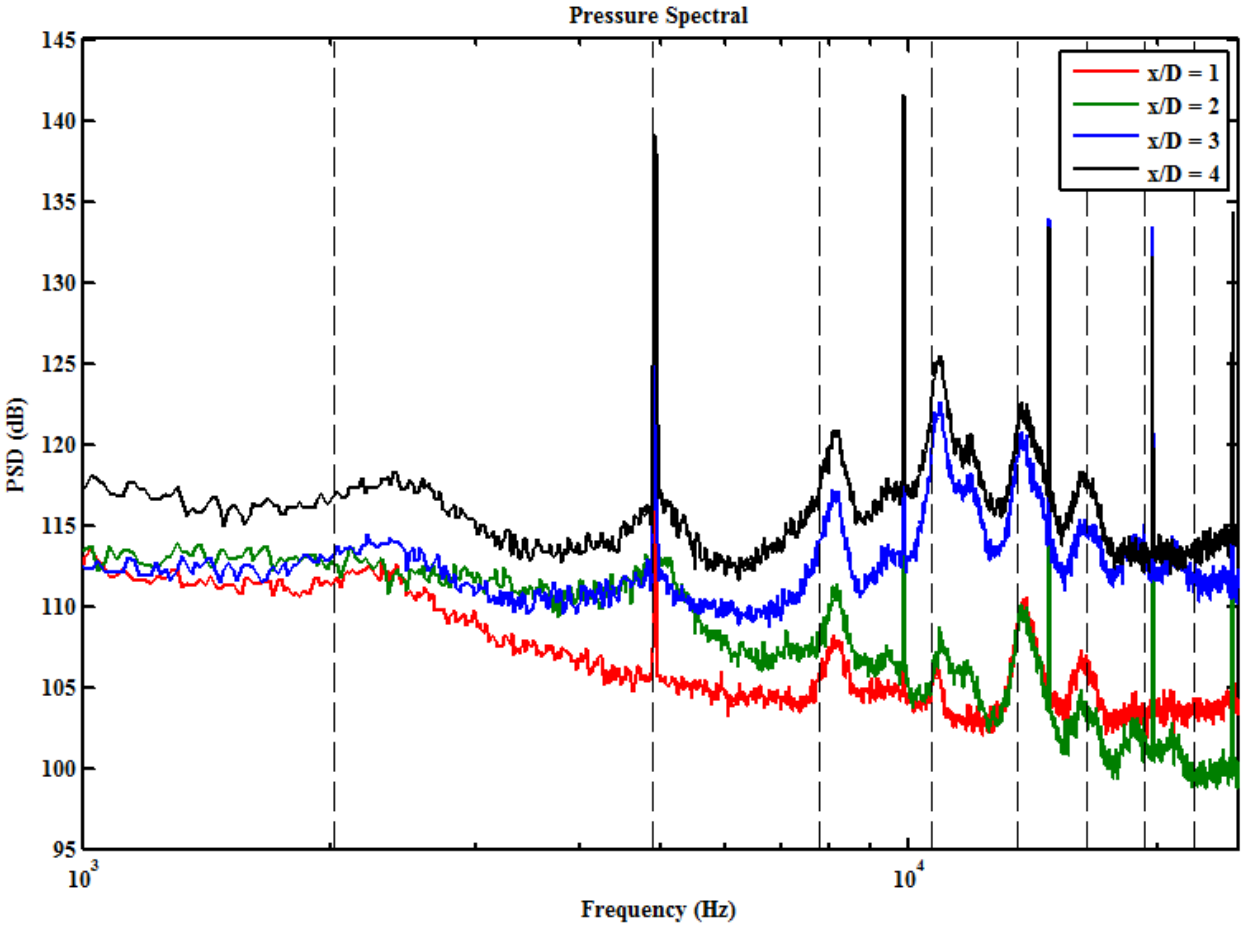

(c) 2nd Rossiter Frequency Excitation

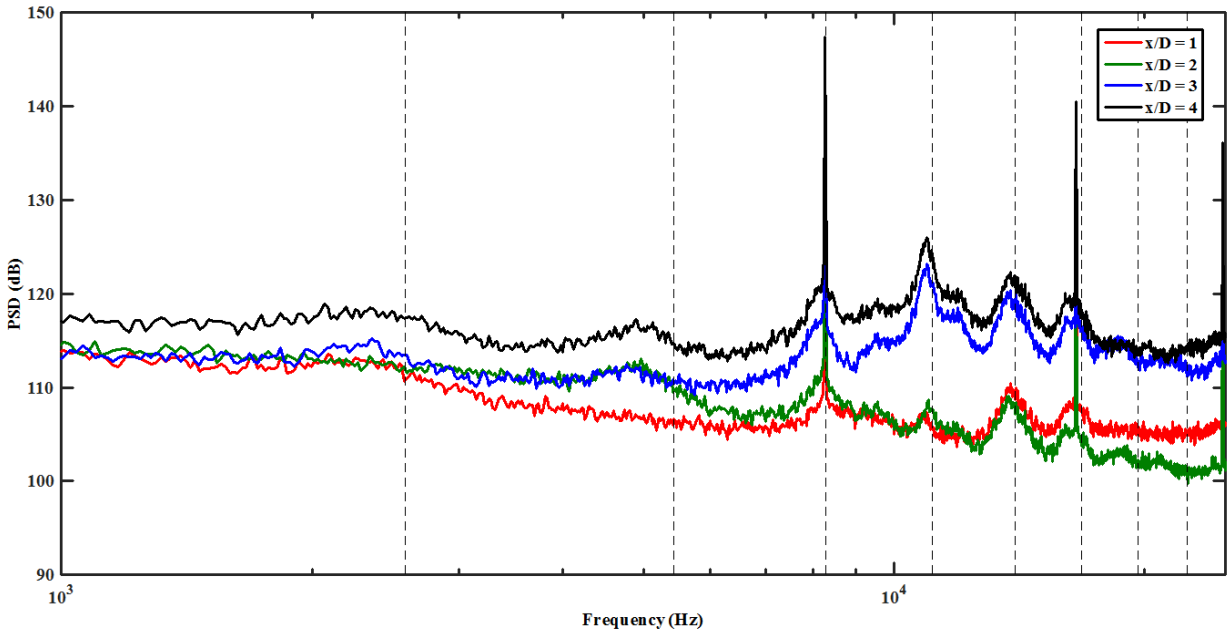

(d) 3rd Rossiter Frequency Excitation

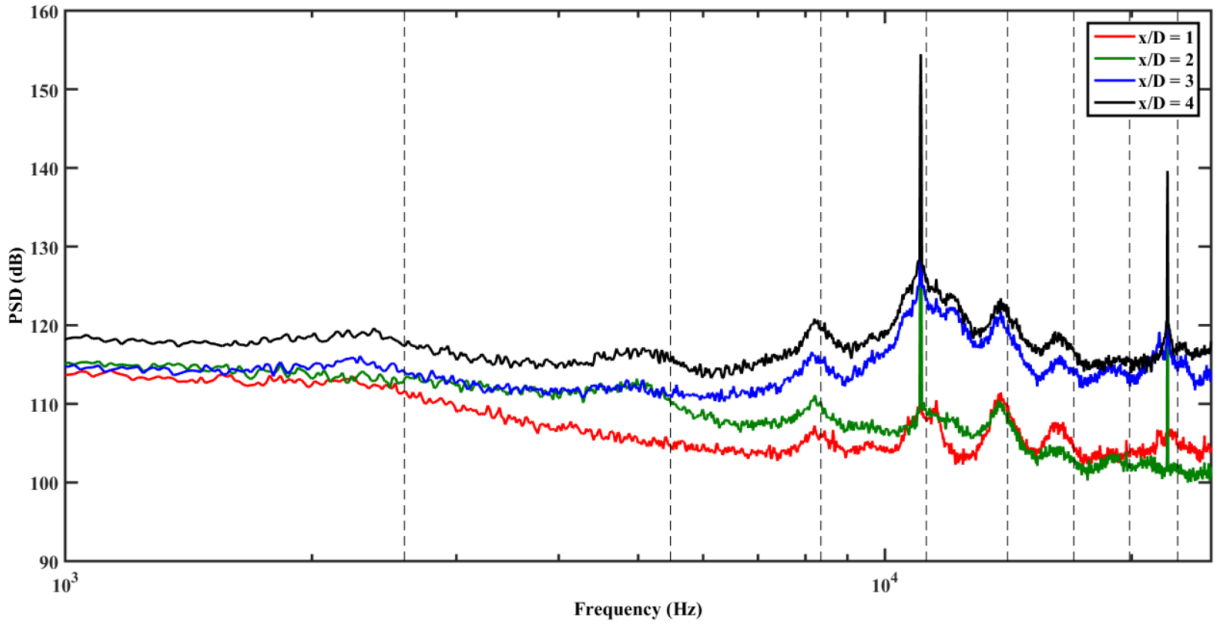

(e) 4th Rossiter Frequency Excitation

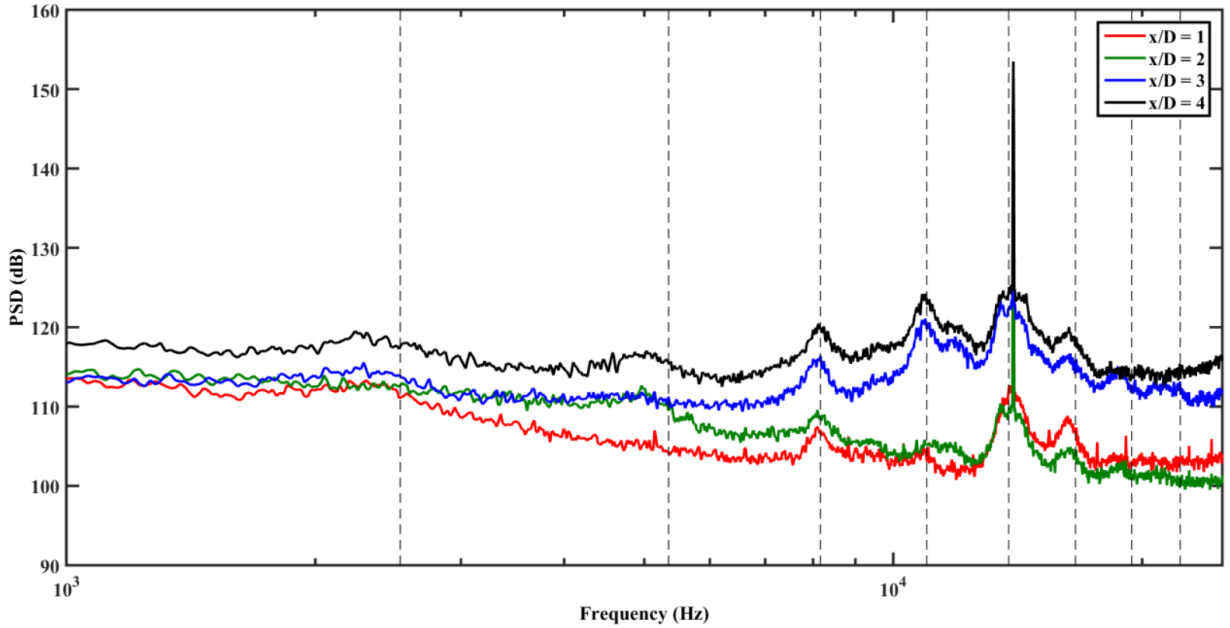

(f) 5th Rossiter Frequency Excitation

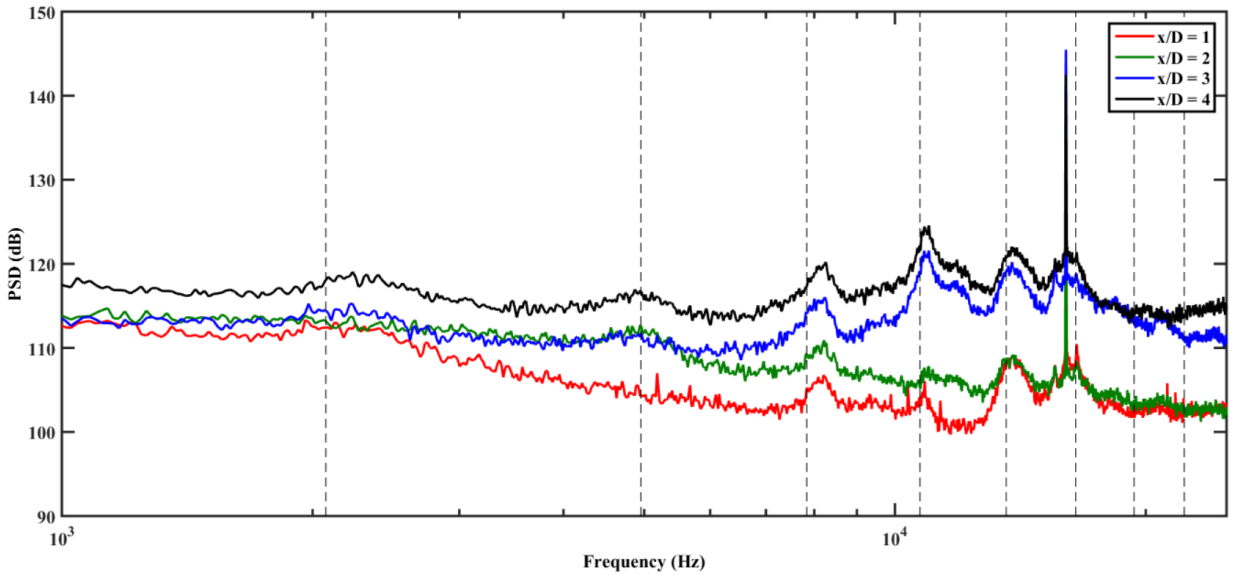

(g) 6th Rossiter Frequency Excitation

Figure 12: Excitation from below 1st Rossiter Frequency to above 6th

From Figure 12 it can be inferred that the 4th Rossiter mode showed some evidence of being enhanced. The first two Rossiter modes aren't naturally strongly resonating; thus the peaks are shorter and rounder. From the preceding modes, the 4th Rossiter mode is the dominant mode. Though the resonance is weak, this may provide the actuators enough resonance to enhance.

After the refined frequency sweep, plots of the difference between the baseline and the excited PSD were generated to help determine where resonance enhancement could be observed. Figure 13 is a plot of the difference between the difference and the baseline spectra. The Y-axis is the excitation frequency where excitation occurs and the X-axis is the flow frequency. Figure 13 is a plot of the initial coarse frequency sweep. Figure 13 was generated using numerous spectral difference plots stacked together so correlations between resonance and excitation frequency can be easily observed. The observed vertical blue lines indicate that the actuators are suppressing resonance at the Rossiter modes. The presence of a line at each resonating Rossiter mode indicates that the actuators are suppressing all the active Rossiter modes, with the amplitude of

the suppression being dependent on the natural resonance amplitude. Figure 13 shows that the 3rd to 5th Rossiter modes have stronger suppression as the blue color is much darker in this figure. Moreover, it can be observed from Figure 13 that the resonance suppression is dependent on the mode number and excitation frequency. The dotted diagonal lines visible in the figure mark the excitation frequencies (and harmonics) from below the 1st Rossiter frequency to above the 6th Rossiter frequency; these lines are the EMI peaks. The intersection between the line of excitation frequency and the Rossiter modes represent a coincidence between excitation frequency Rossiter frequencies. These regions are potential regions of amplification. These are potential regions of amplification. As a reminder, x/D is the normalized streamwise location of the pressure transducers. Figure 7 (in Chapter 2) shows a schematic of the cavity arrangement depicting the location of the transducers.

Figure 13 depicts the effect of flow frequency at different excitation frequencies. This data is presented for all 4 channels to provide information regarding the effect of the actuators on the cavity flow at various locations. As shown, in Figure 13, the yellow/reddish spots that signify localized amplification reduce in area moving from one location to the other. For instance, at x/D= 1, the yellow/red spot spread out a lot more as compared to x/D= 4 when the yellow/red spots occupies less regions.

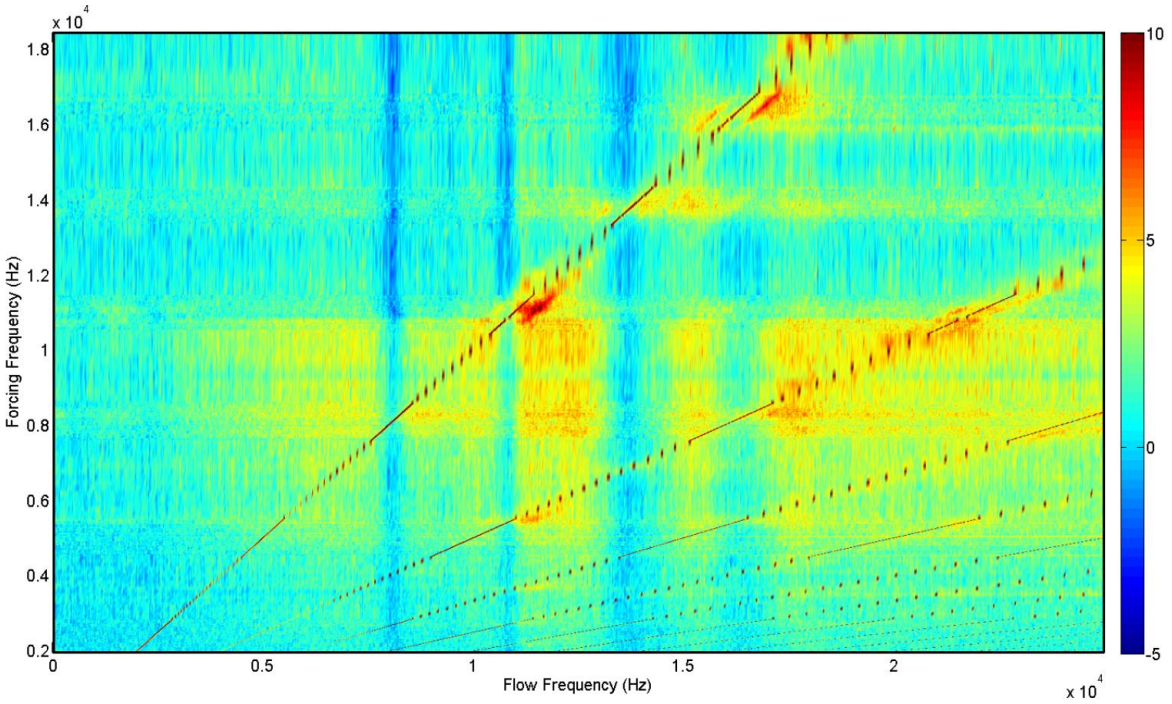
x 10^4
1.8
1.6
1.4
1.2
1
0.8
0.6
0.4
0.2
Forcing Frequency (Hz)
0
0.5
1
1.5
2
Flow Frequency (Hz)
x 10^4
10
5
0
-5

(a) x/D = 1

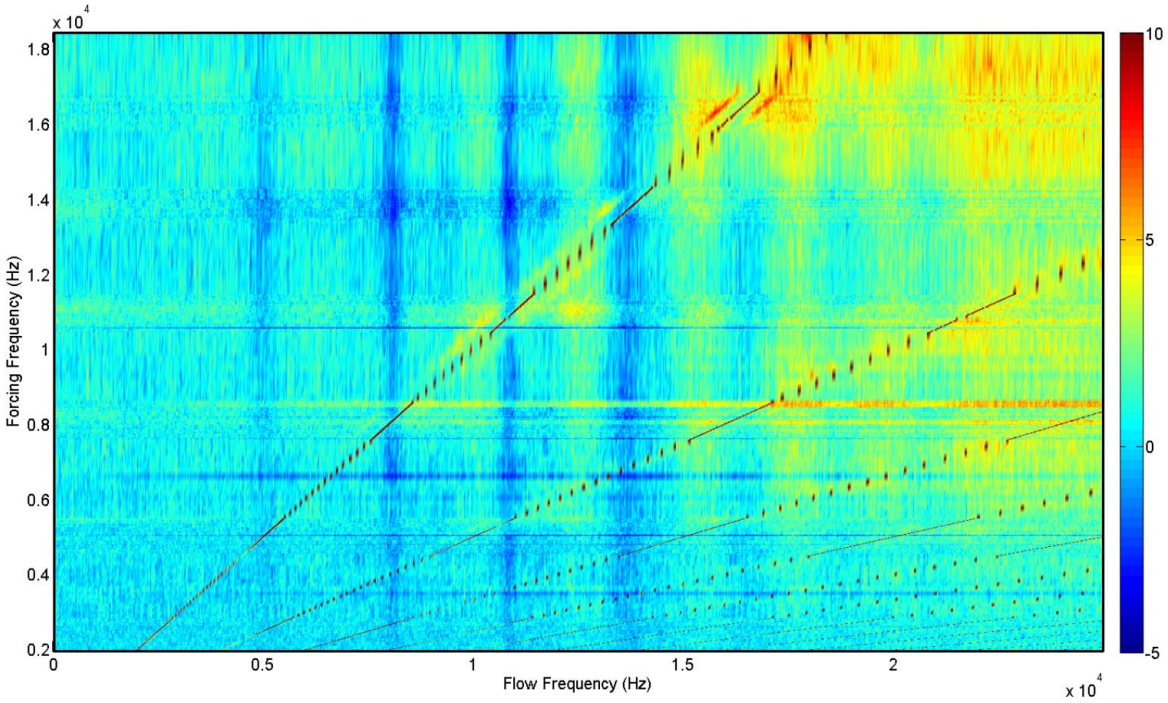
x 10^4
1.8
1.6
1.4
1.2
1
0.8
0.6
0.4
0.2
Forcing Frequency (Hz)
0
0.5
1
1.5
2
Flow Frequency (Hz)
x 10^4
10
5
0
-5

(a) x/D = 2

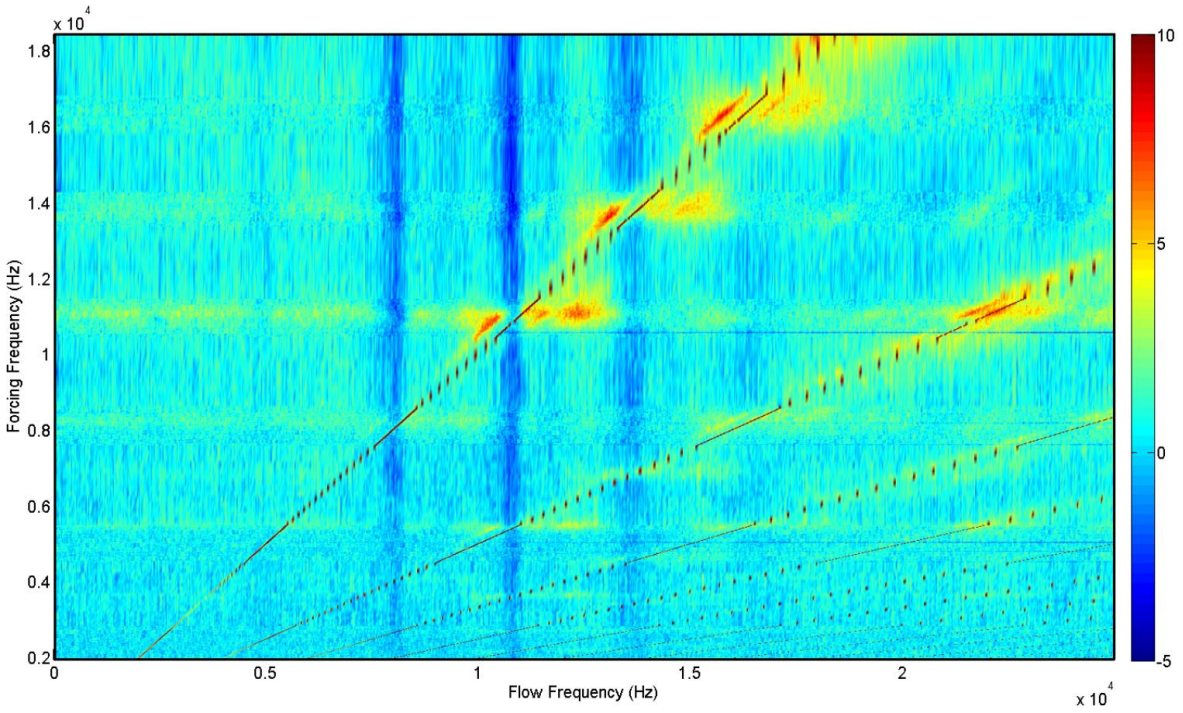

(b) x/D = 3

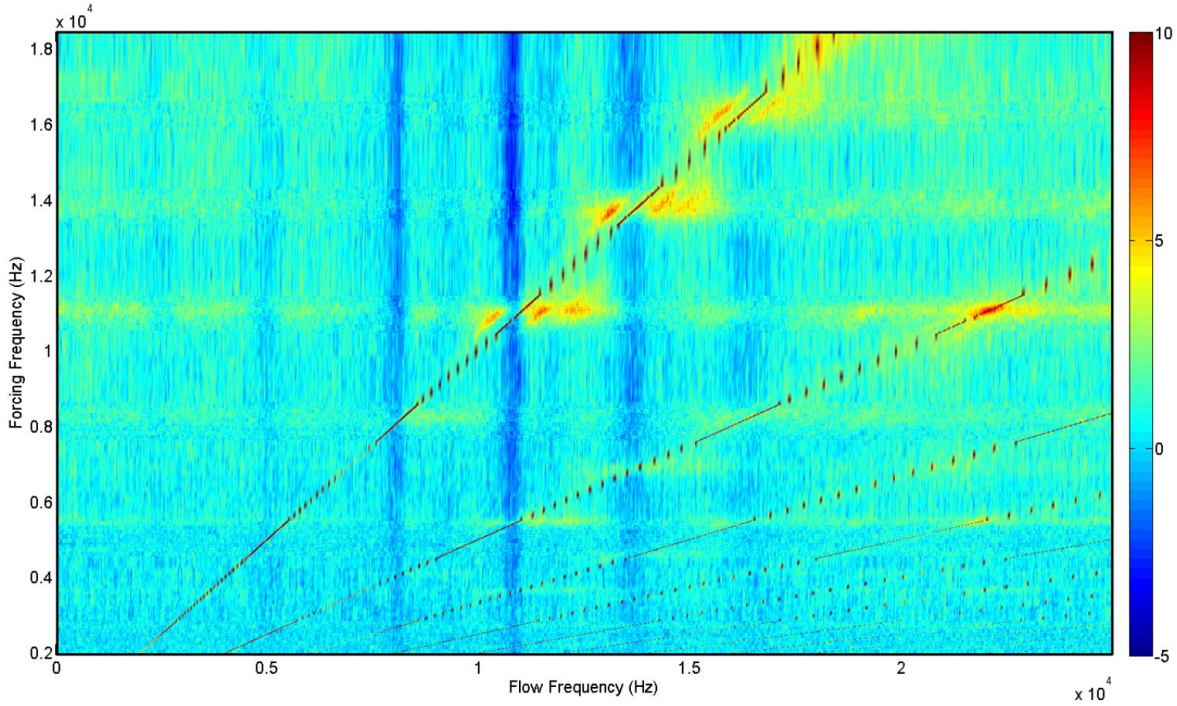

(c) x/D = 4

Figure 13: Spectra for Various Excitation Frequencies

The yellow/red regions in Figure 13 are localized amplification and can be seen near the excitation 1st harmonic when introducing enhancement near the 4th Rossiter frequency. This localized amplification differs with location. Figure 13a shows some localized amplification when introducing enhancement near the 4th, 5th and 6th Rossiter frequency. No obvious enhancement was observed after the coarse frequency sweeps due to the flow not being excited at exactly the right predicted Rossiter Strouhal number. The refined frequency sweep allowed the 4th Rossiter frequency to be better matched to the naturally resonating frequency. The localized amplification noticed near 1st harmonic of the excitation frequency when introducing enhancement near the 4th Rossiter frequency suggests that the plasma actuator can actually enhance resonance in the weak cavity. The resonant peaks look more like flow response, with narrower spikes, but broader, yet stilled localized amplifications. The 1st harmonic is observed rather than the excitation frequency itself, because EMI is blocking the resonant peaked. EMI is contaminating the results but the localized amplification is a promising sign for the future. This is an uncertainty that needs to be addressed so solid conclusions can be drawn regarding the influence of the plasma actuators on the cavity resonance.

Chapter 5: Conclusions and Future Work

It has been proposed that a plasma controlled cavity could help prevent inlet unstart by augmenting the supportable back pressure of a scramjet isolator, thereby reducing the potential for unstart. If unstart can be efficiently prevented, this would increase the performance and efficiency of a scramjet engine. Prior to the cavity's use as a shock trap, the influence on resonance of the cavity of the plasma actuators proposed for control needed to be assessed. The actuators' ability to excite resonance in the cavity is crucial to allowing the cavity to augment the ability of a scramjet isolator in preventing inlet unstart. Cavity resonance leads to high drag penalty, but the cavity resonance is also needed to improve the shock-trapping capabilities of the cavity. Their ability to control the cavity is crucial in this research because resonance must be enhanced by the plasma actuators so a "shock trap" mode can be implemented using a detection algorithm. Spectral data from pressure measurements on the cavity floor led to the choice of a rounded trailing edge with a radius equal to ½ the cavity depth and a cavity length of 2.2 in. (L/D = 4.4) as the optimal cavity geometry. This geometry was selected because the pressure measurements demonstrate that this was a cavity with a weak enough resonance that could be excited by the plasma actuators.

Coarse frequency sweeps showed no resonance enhancement by the plasma actuators so the frequency sweep was refined around predetermined frequencies of interest. The frequencies of interest were normalized by temperature to better match the Rossiter frequencies. These refined sweeps showed some localized amplification near the excitation 1^{st} harmonic when forcing near the 4^{th} Rossiter frequency. This strongly suggests that the LAFPAs are enhancing resonance when they excite the flow at the dominant Rossiter mode. A problem encountered with the actuated measurements was the presence of the EMI during the data collection that made

analysis of the excited cases difficult. Due to this EMI, it is difficult to confidently conclude that the plasma actuators can enhance resonance in the weakly resonating cavity. This is because the EMI overlaps with the tonal peaks that are associated with cavity resonance in key cases, blocking our ability to observe the peak tone amplification.

The next step in this project will be assessing the cavity's shock-trapping capabilities to verify if it could prevent inlet unstart and help improve the performance and efficiency of the scramjet engine. A shock generator will be used to assess the cavity's ability to withstand back-pressure rise. Eliminating EMI will be a major task in the future to get better results and better understanding of where amplification is happening. This will allow concrete conclusion to be drawn regarding the actuators influence on resonance. Once the elimination of EMI is achieved successfully, the capabilities of the plasma controlled cavity to act as a shock trap can be fully assessed.

References

1. Ahuja, K. K., and Mendoza, J., "Effects of Cavity Dimensions, Boundary Layer, and Temperature on Cavity Noise With Emphasis on Benchmark Data to Validate Computational Aeroacoustic Codes," NASA CR-4653, 1955.
2. Caraballo, E., Webb, N., Little, J., Kim, J.-H., and Samimy, M. "Supersonic Inlet Control Using Plasma Actuators." AIAA Paper No. 2009-0924 (2009).
3. Cattafesta, L. N., Garg, S., Choudhari, M., and Li, F., "Active Control of Flow-Induced Cavity Resonance," 28th Fluid Dynamics Conference, AIAA Paper 1997-1804, June–July 1997.
4. Cattafesta, L. N., Song, Q., Williams, D. R., Rowley, C. W., and Alvi, F. S., "Active Control of Flow-Induced Cavity Oscillations," Progress in Aerospace Sciences, Vol. 44, Nos. 7–8, 2008, pp. 479–502. doi:10.1016/j.paerosci.2008.07.002
5. Debiasi,M., and Samimy, M., "Logic-Based Active Control of Subsonic Cavity Flow Resonance," AIAA Journal, Vol. 42, No. 9, 2004, pp. 1901–1909. doi:10.2514/1.4799
6. Debiasi,M., and Samimy, M., "Logic-Based Active Control of Subsonic Cavity Flow Resonance," AIAA Journal, Vol. 42, No. 9, 2004, pp. 1901–1909. doi:10.2514/1.4799.
7. Donbar, J. M., Linn, J. J., Srikant, S., and Akella, M. R., "HighFrequency Pressure Measurements for Unstart Detection in Scramjet Isolators," 46th AIAA/ASME/SAE/ASEE Joint Propulsion Conference and Exhibit, AIAA Paper 2010-6557, July 2010.
8. Heller, H., Holmes, D., and Covert, E., "Flow Induced Pressure Oscillations in Cavities—Physical Mechanisms and Suppression Concepts," Journal of Sound and Vibration, Vol. 18, No. 4, 1971, pp. 545–553. doi:10.1016/0022-460X(71)90105-2.
9. Kegerise, M. A., Spina, E. F., Garg, S., and Cattafesta, L. N., "ModeSwitching and Nonlinear Effects in Compressible Flow Over a Cavity," Physics of Fluids, Vol. 16, No. 3, 2004, pp. 678–686.
10. Keshav, S., Samimy, M., Kim, J.-H., Kastner, J., Adamovich, I., Utkin, Y. , "Development and Use of Localized Arc Filament Plasma Actuators For High-speed Flow Control", *Journal of Physics D: Applied Physics*, vol. 40, 2007, pp. 685-694.
11. Kim, J.-H., Nishihara, M., Adamovich, I., Samimy, M., Gorbatov, S., and Pliavaka, F., "Development of Localized Arc Filament Plasma Actuators for High-Speed and High Reynolds Number Flow Control," Experiments in Fluids, Vol. 49, No. 2, 2010, pp. 497–511. doi:10.1007/s00348-010-0819-y
12. Lawson, S. J., and Barakos, G. N., "Review of Numerical Simulations For High-Speed, Turbulent Cavity Flow," Progress in Aerospace Sciences, Vol. 47, No. 3, 2011, pp. 186–216. doi:10.1016/j.paerosci.2010.11.002
13. Little, J., Debiasi, M., Caraballo, E., and Samimy, M., "Effects of Open Loop and Closed-Loop Control on Subsonic Cavity Flows," Physics of Fluids, Vol. 19, No. 6, 2007, pp. 1–15. doi:10.1063/1.2740302
14. McGregor, O. W. and White, R. A. "Drag of Rectangular Cavities in Supersonic and Transonic Flow Including the Effects of Cavity Resonance." AIAA Journal 8.11 (1970): 1959-1964.
15. NASA Langley Research Laboratory, *Scramjet Engine Schematic*.
16. Rossiter, J. E., "Wind-Tunnel Experiments on the Flow Over Rectangular Cavities at Subsonic and Transonic Speeds," Aeronautical Research Council Report No. 3438, 1964.

17. Rowley, C. W., and Williams, D. R., “Dynamics and Control of HighReynolds-Number Flow over Open Cavities,” Annual Review of Fluid Mechanics, Vol. 38, Jan. 2006, pp. 251–276. doi:10.1146/annurev.fluid.38.050304.092057
18. Samimy, M., Kim, J.-H., Kastner, J., Adamovich, I., Utkin, Y., “Active Control of a Mach 0.9 High Reynolds Number Jet for Noise Mitigation Using Plasma Actuators,” AIAA Journal. Vol. 45,No.4,2007a, pp. 890-901. doi: 10.2514/1.27499
19. Samimy, M., Kim, J.-H., Kastner, J., Adamovich, I., Utkin, Y., “Active Control of High-Speed and High-Reynolds-Number Jets Using Plasma Actuators,” Journal of Fluid Mechanics. Vol. 578,No. 1, 2007b. pp. 305-330.
20. Samimy, M., Kearney-Fischer, M., Kim, J.-H., and Sinha, A., “HighSpeed and High-Reynolds Number Jet Control Using Localized Arc Filament Plasma Actuators,” Journal of Propulsion and Power, Vol. 28, No. 2, 2012, pp. 269–280. doi:10.2514/1.B34272
21. Samimy, M., Kim, J.-H., Kastner, J., Adamovich, I., and Utkin, Y., “Active Control of a Mach 0.9 Jet for Noise Mitigation Using Plasma Actuators,” AIAA Journal, Vol. 45, No. 4, 2007, pp. 890–901. doi:10.2514/1.27499
22. Samimy, M., Debiasi, M., Caraballo, E., Serrani, A., Yuan, X., Little, J., and Myatt, J., “Feedback Control of Subsonic Cavity Flows Using Reduced-Order Models,” Journal of Fluid Mechanics, Vol. 579, May 2007, pp. 315–346. doi:10.1017/S0022112007005204
23. Webb, N., Samimy, M. "Supersonic Cavity Control Using Plasma Actuators." 53rd AIAA Aerospace Science Meeting, 2015-19621, (2015). doi: 10.2514/6.2015-1961
24. Yugulis, K., Hansford, S., Gregory, J., and Samimy, M. "Control of High Subsonic Cavity Flow Using Plasma Actuators," AIAA Journal, Vol. 52, No. 7, (2013), pp. 1542-1554.